Journal of Hazardous Materials 186 (2011) 1088–1096

Contents lists available at ScienceDirect

Journal of Hazardous Materials

journal homepage: www.elsevier.com/locate/jhazmat

Adsorption of chromium(VI) and Rhodamine B by surface modified tannery waste: Kinetic, mechanistic and thermodynamic studies

J. Anandkumar[a], B. Mandal[b,*]

[a] Centre for the Environment, Indian Institute of Technology Guwahati, Guwahati 781039, Assam, India
[b] Department of Chemical Engineering, Indian Institute of Technology, Guwahati 781039, Assam, India

ARTICLE INFO

Article history:
Received 14 July 2010
Received in revised form 27 October 2010
Accepted 25 November 2010
Available online 3 December 2010

Keywords:
Adsorption
Cashew testa
Rhodamine B
Tannery biomass
Chromium(VI)

ABSTRACT

In this study, various activation methods have been employed to examine the potential reuse of tannery residual biomass (TRB) obtained from vegetable tanning process for the removal of Cr(VI) and Rhodamine B (RB) from aqueous solution. The maximum BET surface area (10.42 m^2/g), honey comb pore distribution and uptake of both Cr(VI) and RB were achieved when only 3-fold volume of HCl was used to activate the biomass. The pH and temperature experiment showed that they have considerable impact on the adsorption capacity of the used adsorbent. The presence of other ions (Na^+, Ca^{2+} and NH_4^+) significantly reduces the metal uptake but marginal enhancement in the dye removal was observed when Na^+ and NH_4^+ ions were present in the solution. The equilibrium data fitted satisfactorily with the Langmuir model and monolayer sorption capacity obtained as 177–217 and 213–250 mg/g for Cr(VI) and RB at 30–50 °C, respectively. The sorption kinetics was found to follow the pseudo-second-order kinetic model. The increase in adsorption capacity for both metal and dye with increase in temperature indicates that the uptake was endothermic in nature. The results indicate that the HCl modified TRB (A-TRB) could be employed as a low cost adsorbent for the removal of both Cr(VI) and RB from the aqueous solution including industrial wastewater.

1. Introduction

Many industries such as paper and pulp, cosmetics, paint and pigments, plastics, leather tanning and textile industries generate huge amount of coloured effluent and considerable amount of toxic metals. The discharge of such effluents causes toxicological and aesthetical problems. This also inhibits the sunlight penetration into the inland water surface and therefore, reduces photosynthetic activity of aquatic plants [1,2]. Rhodamine B (RB) and hexavalent chromium are widely used in the above industries. It is harmful when it consumed by human beings and animals, and causes irritation to the skin, eyes and respiratory tract [3,4]. Moreover, its carcinogenicity, reproductive and developmental toxicity, neurotoxicity and chronic toxicity towards humans and animals have been experimentally proven [5–7]. Thus, removal and remediation of this Cr(VI) and dye from the industrial effluents is of significant environmental and commercial importance.

Recently more attention was paid on biomass adsorbents due to its lower cost and higher adsorption capacity towards metals and dyes. It was reported that the adsorption capacity of the biosorbent for metals and dyes could be improved greatly through chemical and physical modification [8–10]. However, literatures on the adsorption of both Cr(VI) and RB using biomass based adsorbents are scarce.

In the present study, an investigation has been carried out to check the reusability of tannery residual biomass (cashew testa sludge-solid waste) as a novel low cost adsorbent to remove the Cr(VI) and Rhodamine B from synthetic wastewater. The generation of TRB from vegetable tanning process creates the solid waste management problem. This study may helps to reduce the cost of waste disposal (recycling) and provide an alternative sorbent to the existing commercial activated carbon to remove the tannery wastewater pollutants such as Cr(VI) and dyes. The influence of principal operational parameters of adsorption such as the effect of pH, influence of other ions, binary system and temperature, was monitored to optimize the sorption process for its possible use as a low-cost adsorbent in the field of wastewater treatment and waste recycling management.

2. Materials and methods

2.1. Preparation of synthetic sample

A stock solution of Cr(VI) and RB (1000 mg/l) was prepared by dissolving appropriate quantity of $K_2Cr_2O_7$ (Merck, India) and Rhodamine B (C.I. 45170, LOBA Chemie, India) in Millipore water. The

* Corresponding author. Tel.: +91 361 2582256; fax: +91 361 2582291.
E-mail address: bpmandal@iitg.ernet.in (B. Mandal).

0304-3894/$ – see front matter © 2010 Elsevier B.V. All rights reserved.
doi:10.1016/j.jhazmat.2010.11.104

chemical structure of RB is illustrated in Fig. S1. The stock solution was shaken for 10 min at 180 rpm to obtain complete dissolution and then suitably diluted with water to get the required initial concentrations (100–350 mg/l). Before mixing the adsorbent, the pH of the solution was adjusted using 0.1 N HCl or 0.1 N NaOH. The pH of the solution was measured by pH meter (Eutech, model: 510).

2.2. Collection and preparation of adsorbent

The cashew husk based tannery residual biomass (TRB) after the vegetable tanning processes was obtained from Amjad Finished Leather Co., at Pernambut, Vellore, India. Initially TRB was air dried in sunlight for 24 h and then washed thoroughly with tap water to remove the adhering dirt. After drying precursor was crushed and sieved in the size range of 600–860 μm. The thermal activation of TRB was done at 500 °C based on the literature information for other adsorbents. The chemical activation of TRB was carried out by HCl in different (w/v) ratio (TRB:HCl) and dried at sunlight for 2–3 days. The chemical activation followed by thermal activation of TRB was done by procedure discussed above. Then the adsorbents which are prepared by HCl were soaked in 2% $NaHCO_3$ to remove the residual acid that was left on the adsorbent. Finally, the adsorbents were dried at 110 °C for 2 h and cooled in a dessicator until further use.

2.3. Adsorption experiment

Adsorption experiments were carried out under batch mode at 30 °C, 40 °C and 50 °C. Initially, the effect of pH on sorption capacity of adsorbate (Cr(VI) or RB) onto TRB was carried out and then the effect of other ions, binary system, temperature and initial concentration of the adsorbates were carried at optimum pH. The pH of each solution was adjusted using required quantity of 1 N HCl (or) 1 N NaOH before mixing the adsorbent. In a set of 250 ml Borosil conical flasks containing adsorbate solution (50 ml) of particular initial concentration was placed. Fixed doses (0.05 g/50 ml) of adsorbent were added to the adsorbate solutions. The pH of the each solution was maintained at optimum condition. Each sample was agitated in an incubating shaker (LabTech, Model LSI-1005R) at a particular temperature. Samples at different time intervals were withdrawn and the supernatant of dye solution was separated by centrifuging (5000 rpm) and the filtrate was analyzed for the residual RB concentration using UV–visible spectrophotometer (Perkin-Elmer, model: Lambdas 45) at the maximum wavelength (λ_{max} = 555 nm) of the dye. Similarly, after completion of every set of experiments the supernatant of metal solution was separated by filtration using Whatman filter paper no. 42 and sample was stored for residual chromium analysis. Final residual metal concentration was directly measured by flame atomic absorption spectrophotometer (AAS) (Varian spectra, AA240) with an air–acetylene flame.

2.4. Adsorbent characterization

Scanning electron microscopy (SEM) (Leo, 1430 vp, Carl Zeiss, German) characterization was carried out to observe the surface texture and porosity for two states of TRB such as TRB without activation and TRB with HCl activation (A-TRB) (1:3, w/v, ratio). To resolve the functional groups and its wave numbers, spectra analysis was done for TRB before and after treatment using Fourier transform infrared spectrometer (FT-IR) (Perkin-Elmer, PE-RXI) in the range of 500–4000 cm^{-1}. In this analysis, finely grounded sorbent was encapsulated with KBr in the ratio 1:20 in order to prepare the translucent sample disks. The BET surface areas and monolayer volumes of the high performance HCl treated TRBs were measured in surface area analyser (Beckman Coulter, SA-3100) using nitrogen adsorption isotherm at −196 °C. Before measurement, the samples were degassed using Helium at 200 °C for 2 h.

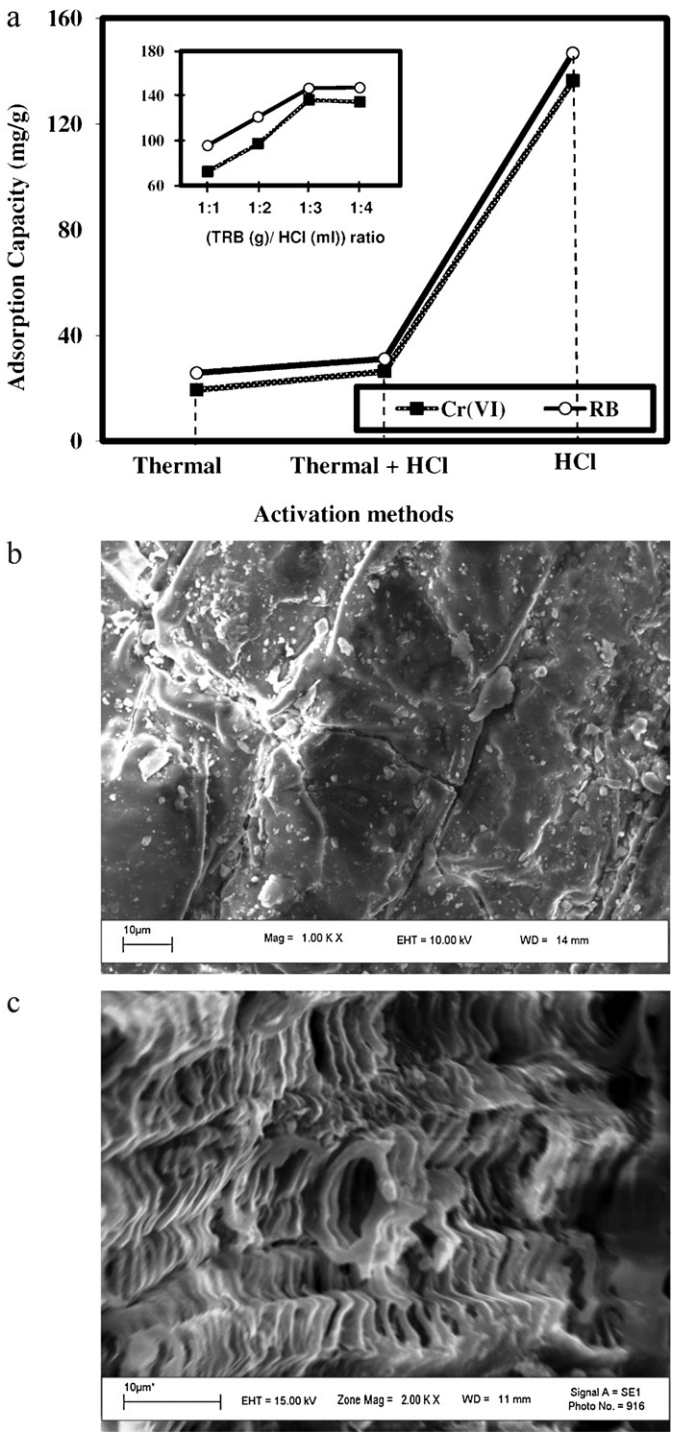

Fig. 1. (a) Effect of different activation methods on sorption capacity of TRB (C_o = 200 mg/l, w = 0.05 g, v = 50 ml, t = 1440 min and T = 30 °C), SEM picture of (b) untreated TRB and (c) HCl treated A-TRB.

3. Results and discussion

3.1. Effect of activation method

The effect of different activation methods on sorption capacity of Cr(VI) or RB onto TRB sorbent is shown in Fig. 1a. The poor sorption capacity for both Cr(VI) and RB was found by thermal activated TRB

Table 1
Physical properties of A-TRB.

Properties	HCl Treated TRB (A-TRB) Impregnation ratio [TRB Weight (g)/HCl volume (ml)]			
	1:1	1:2	1:3	1:4
BET surface area (m^2/g)	3.844	5.868	10.422	9.977
BET mono layer volume (cc/g)	0.8831	1.3481	2.3945	2.2922
Total pore volume (ml/g)	0.0289	0.0343	0.0508	0.0448
Langmuir surface area (m^2/g)	2.705	4.855	8.350	9.237
Langmuir monolayer volume (cc/g)	0.6215	1.1154	1.9184	2.1222

(Cr(VI): 19 mg/g and RB: 26 mg/g) as well as HCl + thermal activated TRB (Cr(VI): 25.2 mg/g and RB: 31 mg/g) due to the greater loss of functional groups as well as the loss of the favorable adsorption sites at higher temperature (discussed in Section 3.2). The effect of chemical ratio on sorption capacity of both Cr(VI) and RB dye is also shown in Fig. 1a. It can be seen from the figure that the sorption capacity of both Cr(VI) and RB increased from 72 mg/g to 136 mg/g and 96 to 146 mg/g as the impregnation ratio (HCl/TRB, w/v) increased from 1:1 to 1:3, respectively. The increase in chemical ratio in TRB activation increased the pore development, surface area (see Section 3.2) and thus, enhanced the sorption capacity of metal and dye. However, beyond 1:3 ratios the sorption capacity remains constant. It may be due to the fact that the number of active binding sites remains unchanged. Therefore, the sorbent which was prepared by only the HCl activation at 1:3 (TRB:HCl) ratio was utilized for the entire study.

3.2. Surface characterization of adsorbent

The effect of impregnation ratio (TRB (g)/HCl (ml)) on BET surface area is presented in Table 1. As given in Table 1, the surface area and total pore volume increases with increase in chemical ratio. This is due to the improvement in surface texture and the pore formation. However, beyond 1:3 impregnations ratio the surface area was slightly decreased. This is may be due to the formation of multi-layer of activating agent at higher chemical ratio. Similar observation has been reported by Mohanty et al. [10].

The SEM image of TRB prior to HCl activation is shown in Fig. 1b. A regular plain surface with no pores on TRB was observed from this figure. The SEM image of TRB after the HCl treatment is shown in Fig. 1c. The progressive change and well developed honeycomb structured pores on the surface of the A-TRB were observed from this figure.

The FT-IR spectra of native TRB are shown in Fig. 2. The bands of raw TRB at 3414, 2927, 1640, 1108, and 1019 cm^{-1} are the stretching vibrations of the surface hydroxyl group (O–H), symmetric vibrations of C–H predominantly for aliphatic acids, COO and C=C groups, C–O stretch and stretching vibrations of C–O–C and $-OCH_3$ (indicative of lignin structure), respectively. The other bending vibrations less than 823 cm^{-1} are the finger print zone that indicates the phosphate functional groups [11]. But, the band frequencies of the above functional groups were not well established for thermal treated and HCl + thermal treated TRB. Some of the fundamental peaks of TRB were shifted from its position after HCl treatment. It might be due to the formation of active sites on the surface of A-TRB by HCl. The peak shifting before and after HCl treatment is represented in Fig. 2. The surface hydroxyl, carboxyl, lignin and phosphate functional groups present in the merely HCl treated TRB were responsible for the metal and cationic RB molecule adsorption due to the electrostatic attraction (discussed in Section 3.9) between the oppositely charged functional groups of A-TRB [12,13].

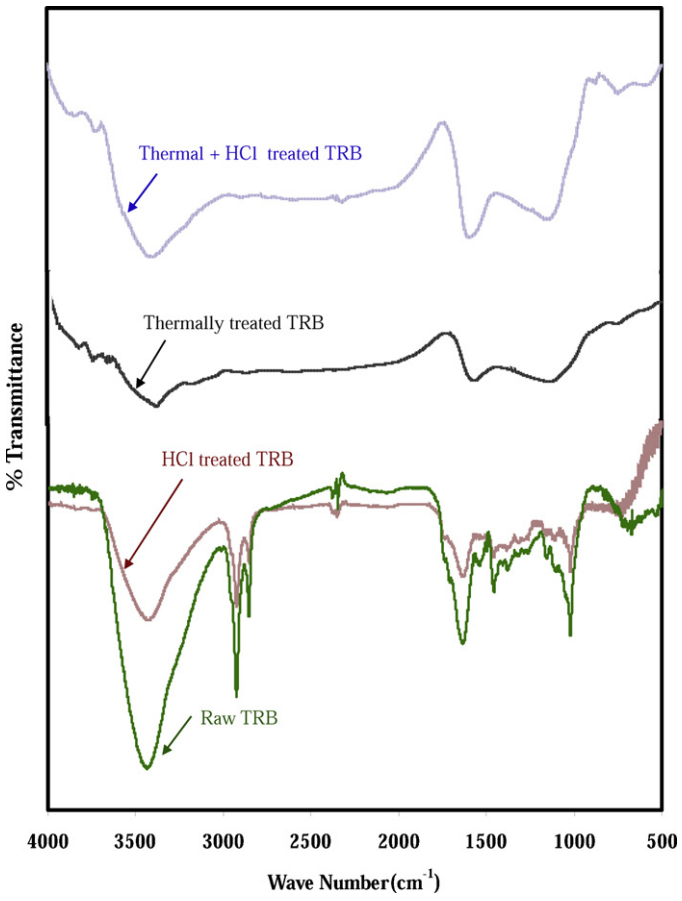

Fig. 2. FT-IR spectra of untreated TRB, thermal treated TRB, HCl with thermal TRB and HCl treated TRB.

3.3. Effect of pH

3.3.1. Effect of pH on Cr(VI) adsorption

One of the most important process parameter for the adsorption of metal and dye on TRB is the pH of the solution. The pH of the solution was varied in the range of 1–11 keeping all other parameters constant. The maximum removal of Cr(VI) was occurred at initial pH 2.0 for A-TRB (Fig. 3). At lower pH the surface area

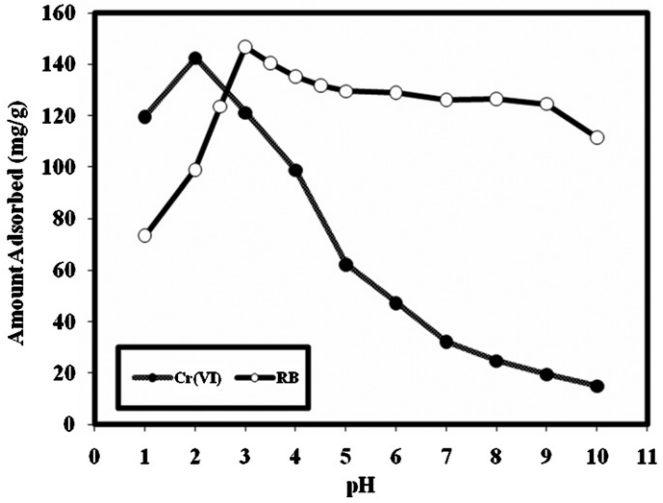

Fig. 3. (a) Effect of pH on sorption capacity of A-TRB: (C_o = 200 mg/l, w = 0.05 g, v = 50 ml, t = 1440 min and T = 30 °C).

of the adsorbent was more protonated and competitive negative ions adsorption occurred between positive surface ($-OH^+$) and free chromate ion. Adsorption of Cr(VI) at pH 2.0 shows the bind of the negatively charged chromium species ($HCrO_4^-$) occurred through electrostatic attraction to the positively charged (due to more H^+ ions) surface functional groups of the adsorbent (discussed in Section 3.9). But in highly acidic medium (pH ≈ 1) H_2CrO_4 (neutral form) is the predominant species of Cr(VI) as reported by Agrawal et al. [14]. Hence, at pH 1.0 percentage adsorption decreased due to the involvement of less number of $HCrO_4^-$ anions on the positive surface. At higher pH due to more OH^- ions adsorbent surface carrying net negative charges, which tend to repulse the metal anions (CrO_4^{2-}) [15]. However, there is also some percentage adsorption at pH > 2.0 but the rate of adsorption is reduced. Above pH 2.0, the net positive charge on the surface of the adsorbent decreased and hence lowered the adsorption capacity of negatively charged adsorbent (CrO_4^{2-}) [16,17]. However, when the reaction pH increased above 2.0, adsorption of Cr^{3+} (formed due to the adsorption couple reduction) might increase because of gradual increase in negative charge on adsorbent surface. But the adsorption-coupled reduction of Cr(VI) to Cr(III) was less above pH 2.0 due to the less adsorption of $HCrO_4^-$ (discussed in Section 3.9). At pH ≈ 8.0, CrO_4^{2-} is the predominant form and repulsion take place by high negative surface [15].

3.3.2. Effect of pH on RB adsorption

There was a sharp increase in sorption capacity (34.39–146.80 mg/g) with increase in pH of the RB solution from 2 to 3.5 as shown in Fig. 3. At very low pH (2.0), the surface of the sorbent was more protonated (due to more H^+ ions). As the pH increased from 2.0 to 3.5, the availability of $-OH^-$ group increased. Also, below pH 3.5 RB molecules remain in monomeric form and dye molecule can easily enter into the pore structure of the adsorbent [18]. Hence, sorption capacity increases with increase in solution pH up to 3.5. However, above pH 3.5 the sorption capacity of RB decreased from 146.80 to 111.48 mg/g. The pH higher than 3.5, zwitterionic form of RB in the water might increased the aggregation of RB (bigger molecules) and thus unable to enter into the pore structure on the surface. The maximum sorption capacity of RB was 146.80 mg/g at pH 3.5. Thus, all further RB studies were carried out at pH 3.5.

3.4. Effect of other ions (Na^+, Ca^{2+} and NH_4^+) in test solution

The influence of other co-ions such as Na^+, Ca^{2+}, and NH_4^+, which are commonly present in water and wastewater, on the percentage adsorption of both Cr(VI) and RB dye by A-TRB was investigated separately with varying initial concentrations of these ions *viz*., 0, 0.5, 1.0, 5.0, 10 and 20 g/l by keeping both Cr(VI) and RB dye concentration constants (200 mg/l). The effect of other ions on percentage adsorption of Cr(VI) and RB dye sorption on A-TRB is shown in Fig. 4a and b, respectively. Results clearly depict that the percentage adsorption of Cr(VI) decreased when other cations were simultaneously present in the metal solution. Fig. 4a shows that the Cr(VI) adsorption is about 73% in the absence of other ions. However, the sorption capacity of Cr(VI) decreased with increase in the concentration of other ions such as NH_4^+ and Ca^{2+}. At a concentration of 20 g/l of Na^+ and Ca^{2+}, the removal of Cr(VI) was about 55%. Fig. 4b depicts that the addition of Ca^{2+} did not change the RB dye sorption capacity A-TRB. Nevertheless, the presence of both Na^+ and NH_4^+ slightly improved the RB dye adsorption capacity onto A-TRB.

3.5. Effect of binary system

A study to assess the change in metal and dye sorption capacity of A-TRB was conducted at various favorable pH conditions

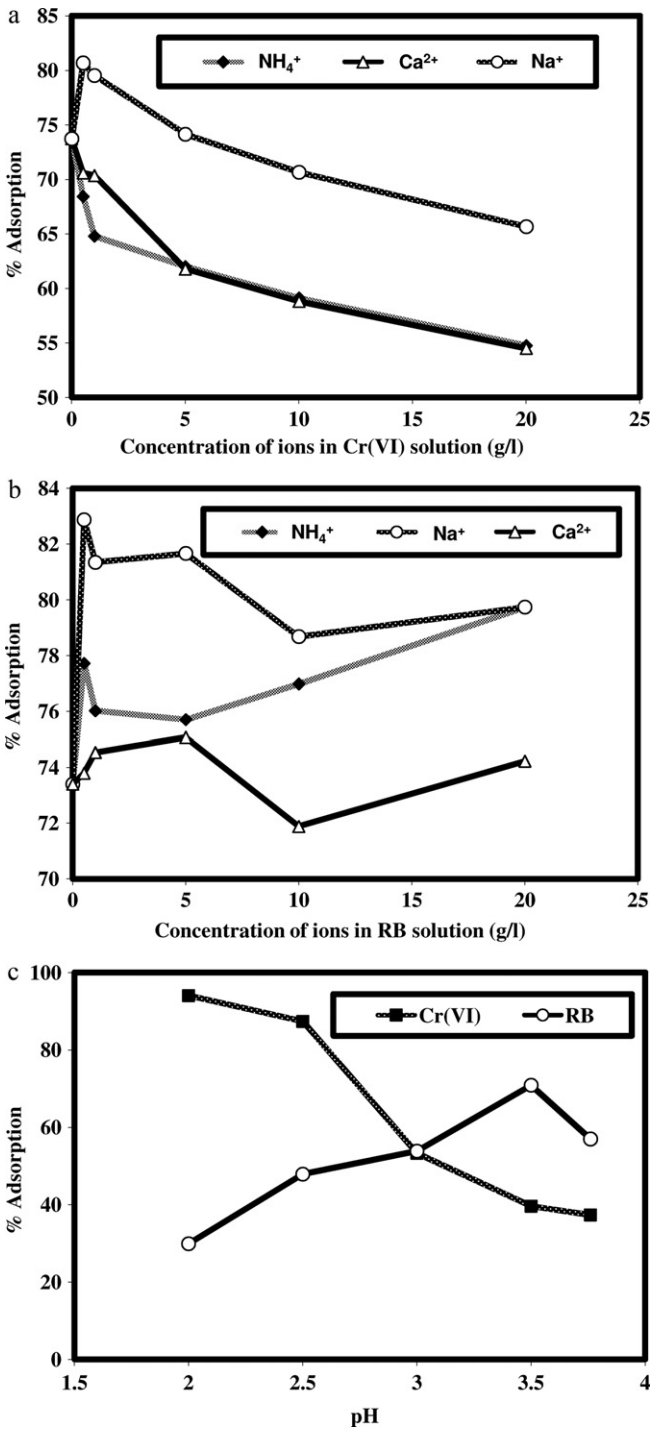

Fig. 4. (a) Effect of other ions on sorption of Cr(VI) onto A-TRB: (C_o = 200 mg/l, pH = 2.0, w = 0.05 g, v = 50 ml, t = 1440 min and T = 30 °C). (b) Effect of other ions on sorption of RB onto A-TRB: (C_o = 200 mg/l, pH = 3.5, v = 50 ml, w = 0.05, t = 1440 min and T = 30 °C). (c) Effect of binary sorption system onto A-TRB at different pH: (C_o = 150 mg/l of Cr(VI) and 150 mg/l of RB, v = 50 ml, w = 0.05, t = 1440 min and T = 30 °C).

when these two were mixed together. An equal mixed binary concentration of 150 mg/l of metal and 150 mg/l of dye solution was used in this study. More than this proportion makes the precipitation of metal–dye complex. It was observed from Fig. 4c that the adsorption of Cr(VI) decreased from 94 to 37% when pH of the binary solution increased from 2.0 to 3.76 (natural pH), whereas percentage of RB adsorption increased from 30 to 71. The unit adsorption capacity of Cr(VI) on A-TRB at pH

Table 2
Isotherm constants for adsorption of Cr(VI) and RB onto A-TRB.

Solution temperature	Langmuir constants			Freundlich constants			Temkin constants			Halsey constants		
	Q_o (mg/g)	b (l/mg)	R^2	K_f (mg/g)	$1/n$	R^2	A (l/g)	B	R^2	K_h	$1/n$	R^2
30 °C												
Cr(VI)	177.31	0.0698	0.9918	66.8452	0.1807	0.9881	7.0656	22.8980	0.9709	9.4357×10^{-11}	0.1807	0.9881
RB	212.77	0.0548	0.9952	48.0065	0.2844	0.9746	1.0366	38.978	0.9878	1.23×10^{-6}	0.2844	0.9872
40 °C												
Cr(VI)	200.40	0.1090	0.9994	65.5994	0.2275	0.9935	3.1632	32.4301	0.9917	1.0340×10^{-8}	0.2275	0.9935
RB	227.27	0.0911	0.9932	68.7860	0.2347	0.9601	3.2007	34.802	0.9767	1.48×10^{-8}	0.2345	0.9799
50 °C												
Cr(VI)	217.39	0.1126	0.9977	74.2489	0.2141	0.9907	5.4769	31.2463	0.9940	1.8286×10^{-9}	0.2141	0.9907
RB	250	0.1504	0.9943	87.4380	0.2191	0.9613	7.5800	35.154	0.9748	1.38×10^{-9}	0.2191	0.9805

2.0, 2.5, 3.0, 3.5 and 3.76 also decreased from 141.08, 131.09, 79.92, 59.43 and 56.03 mg/g, respectively. But the unit adsorption capacity of RB dye on A-TRB at pH 2.0, 2.5, 3.0 and 3.5 increased and thereafter at pH 3.76 decreased from 44.86, 71.85, 80.78 and 106.29 and 85.46 mg/g, respectively. The reasons are discussed already in Section 3.3. However, the overall sorption capacity of the adsorbent increased in binary system than that of single solution system.

3.6. Isotherm studies

In order to optimize the design of an adsorption system, analysis of the adsorption equilibrium data is important. Four isotherm equations namely the Langmuir, Freundlich Temkin and Halsey isotherm models were tested for the sorption phenomenon of Cr(VI) and RB onto A-TRB.

The Langmuir equation was chosen to estimate the maximum adsorption capacity corresponding to complete monolayer coverage on the homogenous adsorbent surface without any interaction between adsorbed ions. The linerized form of Langmuir equation is commonly represented as

$$\frac{C_e}{q_e} = \left(\frac{1}{Q_o b}\right) + \left(\frac{C_e}{Q_o}\right) \quad (1)$$

where q_e is the amount of adsorbate adsorbed per unit mass of adsorbent in (mg/g), C_e is the retained adsorbate concentration at equilibrium (mg/l), Q_o is a measure of adsorption capacity expressed in (mg/g), and b is the Langmuir constant which is a measure of energy of adsorption expressed in (l/mg). The plots of C_e/q_e versus C_e at the different temperatures are shown in Fig. S2a. It can be observed from this figure that the data were fitted well by straight lines in all cases. The values of regression coefficients obtained at different temperatures are presented in Table 2. The values of Q_o at various temperatures are also included in Table 2. The monolayer sorption capacity of Cr(VI) and RB dye on other adsorbents which are reported in the recent studies are presented in Table 3. Compare to these reported adsorbents our studied adsorbent shows the higher adsorption capacity even at higher range of concentration of both Cr(VI) and RB dye. The essential characteristics of Langmuir isotherm can be described by a separation factor or equilibrium constant R_L, which is represented by:

$$R_L = \left(\frac{1}{1 + bC_o}\right) \quad (2)$$

where C_o is the initial concentration of adsorbate (mg/l) and b is the Langmuir constant. The separation factor (R_L) indicates the isotherm shape and whether the adsorption is favorable or not. If $R_L = 0$, adsorption is irreversible; $0 < R_L < 1$, adsorption is favorable; $R_L = 1$ adsorption is linear and $R_L > 1$ adsorption is unfavorable. The R_L factor for different initial concentrations of Cr(VI) or RB dye adsorption onto A-TRB obtained in this work was in the range of $0 < R_L < 1$. Those R_L values were in very good agreement with the reported values in the literature [24].

The Freundlich empirical equation, which is based on heterogeneous surface and infinite surface coverage, was chosen to analyze the equilibrium data. The linerized form of Freundlich equation is commonly represented by:

$$\log q_e = \log K + \frac{1}{n}\log C_e \quad (3)$$

Table 3
Comparison of maximum monolayer adsorption of Cr(VI) and RB on various adsorbents.

Adsorbents	Adsorption capacity (mg/g)	pH	Concentration range (mg/l)	References
Cr(VI)				
Saw dust	41.52	1.0	100–400	[19]
Leersia hexandra Swartz biomass	2.45	2.0	5–25	[20]
Ulva lactuca alga and its activated carbon	10.61 and 112.36	~1.0	5–50 and 75–250	[21]
Pine needles	5.36	2.0	100	[22]
Eucalyptus bark	45.0	2.0	250	
Coconut husk fibres	29.0	2.1	80	
Terminalia arjuna nuts activated carbon	28.4	1.0	10–30	[7]
Sawdust of Sal tree activated carbon	9.55	3.5	40	
Tamarind hull activated carbon	85.91	2.0	25–75	
Bael fruit shell activated carbon	17.27	2.0	50–125	
A-TRB	177.31–217.39	2.0	100–350	Present study
RB				
Treated parthenium biomass	59.2	7.0	50–250	[12]
Surfactant modified coconut coir pith	14.9–16.45	9.2	20–100	
Activated carbon	400	–	48	
Bagasse pith activated carbon	93.1–103.6	3.5	100–600	[23]
H_2SO_4 acid activated sludge	7.181	6.5	0.72 μmol/l	[9]
Carbonaceous industrial waste	91.1	5.5	48	[4]
Sago waste carbon	16.2	5.7	10–40	[8]
A-TRB	212–250	3.5	100–350	Present study

Table 4
Kinetic constants for Cr(VI) and RB adsorption onto A-TRB.

Initial adsorbate concentration (mg/l)	Pseudo-first-order model					Pseudo-second-order model			
	$q_{e,exp}$ (mg/g)	K_{ad} (l/min)	$q_{e,cal}$ (mg/g)	R^2	χ^2	k' (g/mg/min)	$q_{e,cal}$ (mg/g)	R^2	χ^2
100									
Cr(VI)	93.03	0.0193	88.70	0.9390	0.2154	5.16×10^{-4}	96.15	0.9968	0.1042
RB	89.32	0.0030	49.78	0.9743	31.4764	1.25×10^{-4}	93.34	0.9998	0.1741
150									
Cr(VI)	119.89	0.0141	94.93	0.9552	6.8627	2.87×10^{-4}	126.58	0.9981	0.3536
RB	126.42	0.0023	87.34	0.8983	17.5862	4.49×10^{-5}	136.99	0.9912	0.8156
200									
Cr(VI)	136.45	0.0136	98.86	0.9773	14.2930	2.53×10^{-4}	144.93	0.9988	0.4962
RB	146.8	0.0016	68.64	0.9166	89.0004	4.86×10^{-5}	153.85	0.9926	0.3231
250									
Cr(VI)	145.40	0.0131	80.91	0.9846	51.4023	3.4×10^{-4}	151.52	0.9995	0.2472
RB	172.74	0.0018	99.59	0.9229	53.7295	3.03×10^{-5}	185.19	0.9924	0.8370
300									
Cr(VI)	154.83	0.0145	89.23	0.9818	48.2277	3.8×10^{-4}	161.29	0.9990	0.2587
RB	182.33	0.0021	96.81	0.9451	75.5466	3.56×10^{-5}	196.08	0.9967	0.9642
350									
Cr(VI)	174.25	0.0157	122.80	0.9577	21.5562	2.5×10^{-4}	185.19	0.9993	0.6463
RB	196	0.0021	118.22	0.9360	51.1735	2.77×10^{-5}	212.77	0.9956	1.3218

where q_e is the amount of adsorbate adsorbed per unit weight of the sorbent (mg/g) and C_e is retained concentrations of adsorbate at equilibrium (mg/l), K is the measure of adsorption capacity and $1/n$ is the adsorption intensity. The plots of $\log q_e$ versus $\log C_e$ at different temperatures are shown in Fig. S2b. It can be observed from this figure that the data were not well fitted by straight lines compared to Langmuir plots. The values of $1/n$ and K obtained at different temperatures are also included in Table 2.

Temkin isotherm model assumes that the heat of adsorption of all the molecules in the layer would decrease linearly with coverage due to adsorbate/adsorbent interactions [25]. The linerized form of Temkin isotherm is commonly represented by:

$$q_e = B \ln A + B \ln C_e \tag{4}$$

where $RT/b = B$, R is the gas constant (8.13 J/mol K) and T (K) is the absolute temperature. The constant B is related to the heat of adsorption; A is the equilibrium binding constant (l/min) corresponding to the binding energy. A plot of q_e versus $\ln C_e$ yields a linear line, as shown in Fig. S2c. The constants A and B are also given in Table 2. The good linear fitting by higher correlation coefficients indicated that there is good interaction between the adsorbate and the adsorbent.

The Halsey isotherm model is suitable for multilayer adsorption. The linerized form of Halsey isotherm is commonly represented by:

$$\ln q_e = \left[\frac{1}{n} \ln K_h\right] - \frac{1}{n} \ln C_e \tag{5}$$

where k_h and n are the Halsey isotherm constant and exponent, respectively. The plot of $\ln q_e$ versus $\ln C_e$ (Fig. S2d) shows the experimental data and the linear form of Halsey model. The Halsey isotherm parameters are presented in Table 2. The good fitting of the Halsey isotherm equations indicates the heteroporosity (i.e., macropore and micropore) of the A-TRB [26]. Among the above four models, Langmuir isotherm model best fitted the experimental data with high R^2 value.

3.7. Sorption kinetics

In order to investigate the adsorption kinetics of Cr(VI) and RB dye onto A-TRB, two models such as pseudo-first order and pseudo-second-order models were used.

The integral form of pseudo-first-order kinetic model proposed by Lagergren is

$$\log(q_e - q_t) = \log q_e - \frac{K_{ad}}{2.303} t \tag{6}$$

The linerized-integral form of the pseudo-second-order model is expressed as:

$$\frac{t}{q_t} = \left(\frac{1}{k' q_e^2}\right) + \frac{t}{q_e} \tag{7}$$

where q_e is the amount of metal or dye adsorbed at equilibrium per unit weight of adsorbent (mg/g), q_t is the amount of solute adsorbed at any time (mg/g), t is the agitation time (min) and K_{ad} and k' are rate constants (Table 4) of pseudo-first-order and pseudo-second-order sorption, respectively. The plots of $\log(q_e - q_t)$ versus t (figure not given) and (t/q_t) versus t (Fig. 5a) were used to determine the rate constants of K_{ad} and k', respectively. In order to identify a suitable kinetic model for the sorption of Cr(VI) or RB on A-TRB Chi-square (χ^2) test analysis has been carried out and also model was considered as good when coefficient of determination (R^2) is high.

$$\chi^2 = \sum \frac{(q_e - q_{em})^2}{q_{em}} \tag{8}$$

where q_e and q_{em} (mg/g) are adsorption capacities of adsorbate at experimental and model value, respectively. The values of χ^2 for kinetic models are also presented in Table 4. The kinetic model that best fits the experimental data with lower χ^2 and high R^2 value for two models was the pseudo-second order model. Moreover, its calculated q_e values were closely fitted with the experimental data. Thus, the pseudo-second-order kinetics was predominant, and that the overall rate of metal as well as dye adsorption process was largely controlled by the chemisorption process.

3.8. Sorption thermodynamics

Thermodynamic parameters such as change in free energy (ΔG°), enthalpy (ΔH°) and entropy (ΔS°) associated to the sorption process were obtained using the following equation:

$$\ln K_d = \frac{\Delta S^\circ}{R} - \frac{\Delta H^\circ}{RT} \tag{9}$$

where R is the universal gas constant (8.314 J/K mol), T is the absolute solution temperature (°C) and K_d is the distribution coefficient. The values of ΔH° and ΔS° were calculated from the slope and

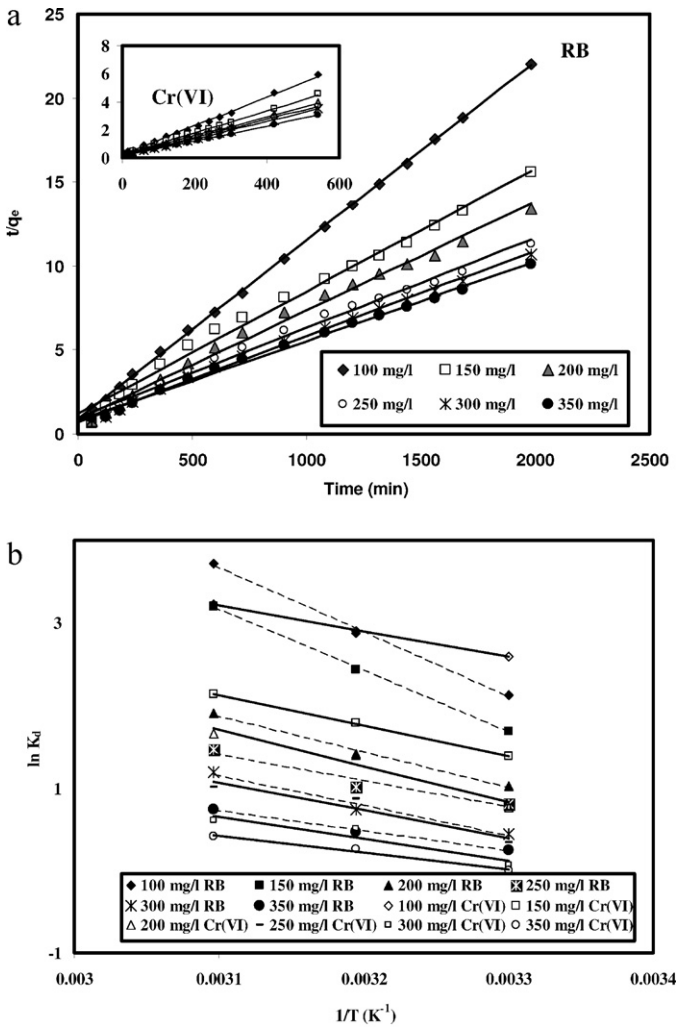

Fig. 5. (a) Pseudo-second-order kinetics plots at 30 °C. (b) Van't Hoff equation plot for the enthalpy change of the sorption process at various initial Cr(VI) and RB concentrations.

intercept of Van't Hoff plot between $\ln K_d$ versus $1/T$ (Fig. 5b) and are listed in Table 5. ΔG° and K_d were calculated using the relation below:

$$\Delta G^\circ = -RT \ln Kd \quad (10)$$

$$K_d = \frac{C_{Ae}}{C_e} \quad (11)$$

where C_{Ae} is amount of the Cr(VI) or RB adsorbed at equilibrium (mg/l) and C_e is retained concentration of each species at equilibrium (mg/l). The negative values of ΔG° increased with increase in temperatures. This indicates the spontaneous nature of the adsorption process. The positive ΔH° values confirmed that the adsorption process was endothermic. The positive value of ΔS° showed the increased randomness at the solid–solution interface during adsorption.

3.9. Adsorption mechanism of Cr(VI) and RB on A-TRB

The change in pH of the solution results in the formation of different ionic species and different adsorbent surface charges [27]. Thus, it is necessary to identify the mechanism of adsorbate uptake by the adsorbent.

Two possible mechanisms such as direct and indirect reduction of Cr(VI) to Cr(III) can be suggested for Cr(VI) removal. In

Table 5
Thermodynamic parameters for adsorption of Cr(VI) and RB onto A-TRB.

Initial RB concentration (mg/l)	ΔH° (J/mol)	ΔS° (J/mol K)	$-\Delta G^\circ$ (J/mol)		
			30 °C	40 °C	50 °C
100					
Cr(VI)	25,830.77	106.7217	6525.93	7530.43	8475.54
RB	64,823.43	231.40	5350.29	7479.06	9770.14
150					
Cr(VI)	30,615.06	112.5827	3480.48	4659.63	5605.76
RB	61,740.6	217.64	4230.17	6326.96	8400.54
200					
Cr(VI)	36,523.52	127.3899	1924.96	3671.02	4355.82
RB	35,908.17	126.75	2556.96	3636.09	4989.71
250					
Cr(VI)	27,872.14	95.21076	829.667	2242.69	2655.07
RB	26,653.85	94.27	2026.93	2605.74	3843.18
300					
Cr(VI)	22,205.31	74.25117	162.121	1314.24	1594.05
RB	30,305.36	103.42	1103.22	1908.70	3112.66
350					
Cr(VI)	16,806.22	55.5988	6.9982	667.105	1090.32
RB	20,307.78	68.92	607.52	1192.19	1947.33

the first mechanism, Cr(VI) is directly reduced to Cr(III) by surface electron-donor groups of the adsorbent and the reduced Cr(III) forms complexes with adsorbent or remains in the solution. But Cr(III) is not adsorbed by adsorbent at pH 2.0. But in the second mechanism, the adsorption-coupled reduction of Cr(VI) to Cr(III) occurred on the adsorbent site itself (Fig. 6a). It consists of three steps; (i) the binding of anionic ($HCrO_4^-$) Cr(VI) to the positively charged groups present on the surface of the adsorbent, (ii) the reduction of adsorbed Cr(VI) to Cr(III) takes place by adjacent electron-donor (CO and O–CH_3) groups of adsorbed sites and (iii) a part of surface reduced Cr(III) is released (Fig. 6a) into the aqueous solution due to the electronic repulsion between the positively charged groups of adsorbent and the surface bound Cr(III). Similar behaviour was observed by Suksabye et al. [28] and Sawalha et al. [29]. At pH 2.0, the reduced chromium is in Cr^{3+} form due to adsorption couple reduction of Cr(VI) and it cannot be adsorbed by positively charged surface of the adsorbent [30,31]. Above pH 2.0, the adsorption of Cr(VI) decreases and hence the release of Cr(III) decreases steadily. Similar behaviour was reported by Dakiky et al. [32] for both Cr(VI) and Cr(III) removal for seven other adsorbents.

The possible mechanism of RB can be explained as follows: as pH decreased below 3.5, the excess H^+ ions neutralize (protonation) the TRB surface bearing –OH^- groups and then it turns to –OH_2^+ site [7,33]. The positive charged surface sites (Fig. 6a) of the sorbent do not favor for cationic dye sorption due to its electrostatic repulsion. At pH 3.5, both surface adsorption and pore diffusion dominates (Fig. 6b) due to the existence of monomeric form of RB molecules. Hence, maximum sorption capacity was observed at pH 3.5. Similar behaviour was observed at pH 3.45 by Guo et al. [18] and Gad and El-Sayed [23]. When pH increased above 3.5, the zwitterionic form of RB in water (Fig. 6c and d) might increase the aggregation of RB to form larger molecules (dimer) and thus unable to enter into the pores. The greater aggregation of zwitterions (neutral) is due to the electrostatic interactions between the carboxyl and xanthene groups (Fig. 6d). The aggregations of RB in water have been reported by Arbeloa and Ojeda [34] and Mchedlov-Petrosyan and Kholin [35]. Hence, at alkaline pH surface sorption only dominates the adsorption process. With increase in temperature the rate of diffusion of the Cr(VI) and RB molecules across the external boundary layer as well as in the interior pores of A-TRB increases due to the decrease in the viscosity of the Cr(VI) or RB solution. This impact might be also due to the enlargement of the pore size or the

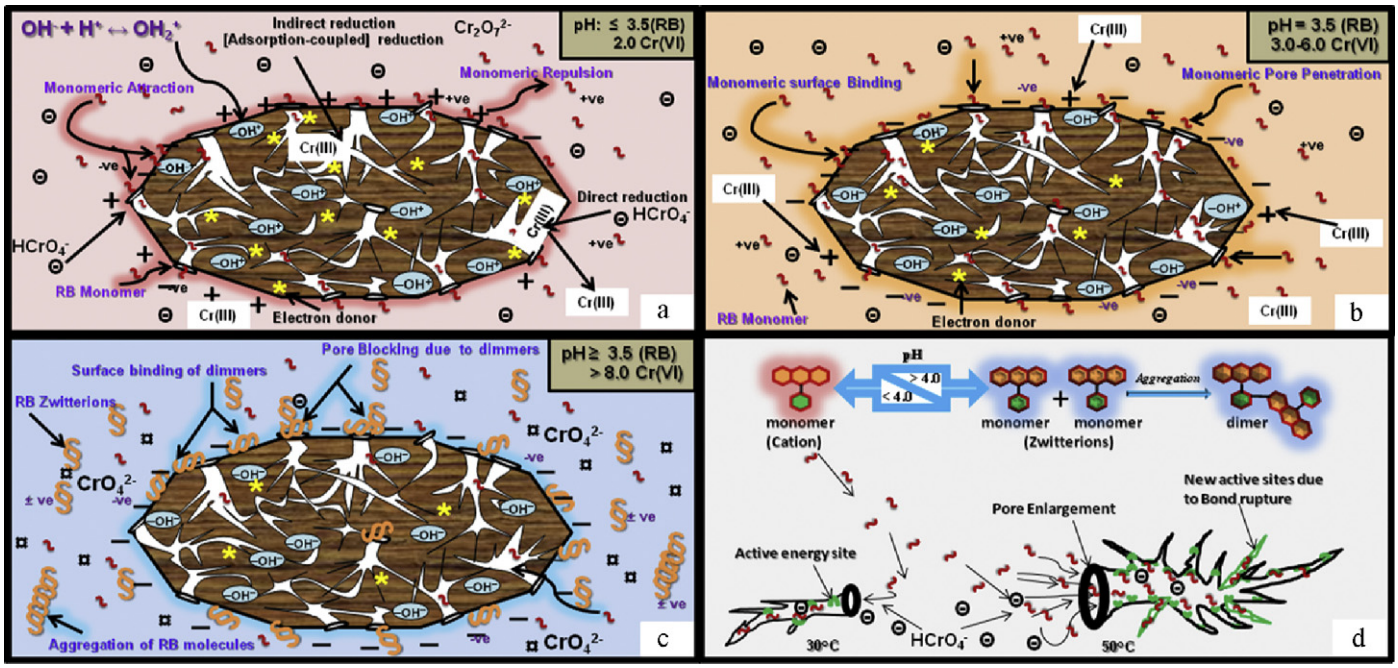

Fig. 6. Adsorption mechanism of Cr(VI) and RB onto A-TRB.

appearance of new adsorption active sites on the adsorbent surface because of the bond rupture (Fig. 6d) while increasing the solution temperature [9,36].

4. Conclusion

This work presents some important phenomena associated with Cr(VI) and Rhodamine B adsorption using tannery residual biomass prepared by different activation methods. Significantly higher sorption capacity of both Cr(VI) and RB by the HCl modified TRB was observed compared to the thermal activated TRB and HCl + thermal activated TRB. The adsorption was found to be strongly dependent on pH, initial adsorbate concentration and solution temperature. The maximum sorption capacity of Cr(VI) and RB was obtained at pH 2.0 and 3.5, respectively. The presence of Na^+ and NH_4^+ ions slightly improved the dye adsorption but Ca^{2+} had no significant effect on RB dye removal. Nevertheless, these three cations considerably reduces the Cr(VI) removal. The equilibrium data were best fitted by Langmuir isotherms than Freundlich, Temkin and Halsey isotherms. Halsey linear regression data showed heteroporosity (i.e., macropore and micropore) of the A-TRB. The equilibrium sorption capacity of both Cr(VI) and RB dye increased with increase in temperature up to 50 °C. This indicates the adsorption process was endothermic. Pseudo-second-order kinetics model was found to be the predominant mechanisms for both metal and dye adsorption onto A-TRB. The thermodynamic parameters associated with the adsorption process were also evaluated. The negative value of ΔG° confirmed the spontaneous nature of both metal and RB sorption onto the A-TRB. The positive ΔH° values confirmed that the adsorption process was endothermic. The above result indicates that A-TRB could be employed as a low cost adsorbent for the removal of both Cr(VI) and RB from the aqueous solution including industrial wastewater.

Appendix A. Supplementary data

Supplementary data associated with this article can be found, in the online version, at doi:10.1016/j.jhazmat.2010.11.104.

References

[1] D. Ozer, G. Dursun, A. Ozer, Methylene blue adsorption from aqueous solution by dehydrated peanut hull, J. Hazard. Mater. 144 (2007) 171–179.
[2] E. Demirbas, M. Kobya, M.T. Sulak, Adsorption kinetics of a basic dye from aqueous solutions onto apricot stone activated carbon, Bioresour. Technol. 99 (2008) 5368–5373.
[3] B. Stephen Inbaraj, J.T. Chien, G.H. Ho, J. yang, B.H. Chen, Equilibrium and kinetic studies on sorption of basic dyes by a natural biopolymer poly (L-glutamic acid), Biochem. Eng. J. 31 (2006) 204–215.
[4] A. Bhatnagar, A.K. Jain, A comparative adsorption study with different industrial wastes as adsorbents for the removal of cationic dyes from water, J. Colloid Interface Sci. 281 (2005) 49–55.
[5] M.F. Boeniger, Carcinogenicity of Azo Dyes Derived From Benzidine, Pub. No. 8-119, Department of Health and Human Services (NIOSH), Cincinnati, 1980.
[6] Kirk-Othomer, Encyclopedia of Chemical Technology, vol. 8, 1994, pp. 547–672.
[7] J. Anandkumar, B. Mandal, Removal of Cr(VI) from aqueous solution using Bael fruit (*Aegle marmelos correa*) shell as an adsorbent, J. Hazard. Mater. 168 (2009) 633–640.
[8] K. Kadirvelu, C. Karthika, N. Vennilamani, S. Pattabhi, Activated carbon from industrial solid waste as an adsorbent for the removal of Rhodamine-B from aqueous solution: kinetic and equilibrium studies, Chemosphere 60 (2005) 1009–1017.
[9] D.J. Ju, I.G. Byun, J.J. Park, C.H. Lee, G.H. Ahn, T.J. Park, Biosorption of a reactive dye (Rhodamine-B) from an aqueous solution using dried biomass of activated sludge, Bioresour. Technol. 99 (2008) 7971–7975.
[10] K. Mohanty, M. Jha, B.C. Meikap, M.N. Biswas, Removal of chromium(VI) from dilute aqueous solutions by activated carbon developed from *Terminalia arjuna* nuts activated with zinc chloride, Chem. Eng. Sci. 60 (2005) 3049–3059.
[11] S. Mohan, G. Sreelakshmi, Fixed bed column study for heavy metal removal using phosphate treated rice husk, J. Hazard. Mater. 153 (2008) 75–82.
[12] J. Yu, B. Li, X. Sun, J. Yuan, R. Chi, Polymer modified biomass of baker's yeast for enhancement adsorption of methylene blue, Rhodamine B and basic magenta, J. Hazard. Mater. 168 (2009) 1147–1154.
[13] S.K. Das, J. Bhowal, A.R. Das, A.K. Guha, Adsorption behavior of Rhodamine B on *Rhizopus oryzae* biomass, Langmuir 22 (2006) 7265–7272.
[14] A. Agrawal, C. Pal, K.K. Sahu, Extractive removal of chromium(VI) from industrial waste solution, J. Hazard. Mater. 159 (2008) 458–464.
[15] B.M.W.P.K. Amarasinghe, R.A. Williams, Tea waste as a low cost adsorbent for the removal of Cu and Pb from wastewater, Chem. Eng. J. 132 (2007) 299–309.
[16] M.M. Mohamed, Acid dye removal: comparison of surfactant modified mesoporous FSM-16 with activated carbon derived from rice husk, J. Colloid Interface Sci. 272 (2004) 28–34.
[17] S.S. Baral, S.N. Das, P. Rath, Hexavalent chromium removal from aqueous solution by adsorption on treated sawdust, Biochem. Eng. J. 31 (2006) 216–222.
[18] Y. Guo, J. Zhao, H. Zhang, S. Yang, J. Qi, Z. Wang, H. Xu, Use of rice husk-based porous carbon for adsorption of Rhodamine B from aqueous solutions, Dyes Pigm. 66 (2005) 123–128.

[19] S. Gupta, B.V. Babu, Removal of toxic metal Cr(VI) from aqueous solutions using sawdust as adsorbent: equilibrium, kinetics and regeneration studies, Chem. Eng. J. 150 (2009) 352–365.
[20] J. Li, Q. Lin, Z. Zhang, Y. Yan, Kinetic parameters of the batch Biosorption of CR(VI) and C(III) onto *Leersia hexangra Swartz* biomass, J. Colloid Interface Sci. 333 (2009) 71–77.
[21] A.E. Sikaily, A.E. Nemr, A. Khaled, O. Abdelwehab, Removal of toxic chromium from wastewater using green alga *Ulva lactuca* and its activated carbon, J. Hazard. Mater. 148 (2007) 216–228.
[22] S.P. Dubey, K. Gopal, Adsorption of chromium(VI) on low cost adsorbents derived from agricultural waste material: a comparative study, J. Hazard. Mater. 145 (2007) 465–470.
[23] H.M.H. Gad, A. El-Sayed, Activated carbon from agricultural by-products for the removal of Rhodamine-B from aqueous solution, J. Hazard. Mater. 168 (2009) 1070–1081.
[24] B.H. Hameed, M.I. El-Khaiary, Sorption kinetics and isotherm studies of a cationic dye using agricultural waste: broad been peels, J. Hazard. Mater. 154 (2008) 639–648.
[25] M. Hosseini, S.F.L. Mertens, M. Ghorbani, M.R. Arshadi, Asymmetrical Schiff bases as inhibitors of mild steel corrosion in sulphuric acid media, Mater. Chem. Phys. 78 (2003) 800.
[26] N.A. Oladoja, I.A. Ololade, J.A. Idiaghe, E.E. Egbon, Equilibrium isotherm analysis of the sorption of congo red by palm kernel coat, Cent. Eur. J. Chem. 7 (4) (2009) 760–768.
[27] Z. Klika, H. Weissmannová, P. Čapková, M. Pospíšil, The Rhodamine B intercalation of montmorillonite, J. Colloid Interface Sci. 275 (2004) 243–250.
[28] P. Suksabye, P. Thiravetyan, W. Nakbanpote, S. Chayabutra, Chromium removal from electroplating wastewater by coir pith, J. Hazard. Mater. 141 (2007) 637–644.
[29] M.F. Sawalha, J.R. Peraita-Videa, G.B. Saupe, K.M. Dokken, J.L. Gardea-Torresdey, Using FTIR to corroborate the identity of functional groups involved in the binding of Cd and Cr to saltbush (*Atriplex canescens*) biomass, Chemosphere 66 (2007) 1424–1430.
[30] H. Li, Z. Li, T. Liu, X. Xiao, Z. Peng, L. Deng, A novel technology for biosorption and recovery hexavalent chromium in wastewater by bio-functional magnetic beads, Bioresour. Technol. 99 (2008) 6271–6279.
[31] M. Uysal, I. Ar, Removal of Cr(VI) from industrial wastewaters by adsorption part I: determination of optimum condition, J. Hazard. Mater. 149 (2007) 482–491.
[32] M. Dakiky, M. Khamis, A. Manassra, M. Mer'eb, Selective adsorption of chromium(VI) in industrial wastewater using low-cost abundantly available adsorbents, Adv. Environ. Res. 6 (2002) 533–540.
[33] T.G. Chuah, A. Jumasiah, I. Azni, S. Katayon, S.Y.T. Choong, Rice husk as a potentially low-cost biosorbent for heavy metal and dye removal: an overview, Desalination 175 (2005) 305–316.
[34] L. Arbeloa, P.R. Ojeda, Dimeric states of Rhodamine B, Chem. Phys. Lett. 87 (1982) 6.
[35] N.O. Mchedlov-Petrosyan, Y.V. Kholin, Aggregation of Rhodamine B in water, Russ. J. Appl. Chem. 77 (2004) 414–422.
[36] R.W. Couglin, F.S. Ezra, Role of surface acidity in the adsorption of organic pollutants on the surface, Environ. Sci. Technol. 2 (1968) 291–297.